Available online at www.sciencedirect.com
SCIENCE DIRECT
Journal of Geodynamics 41 (2006) 234–241
JOURNAL OF GEODYNAMICS
http://www.elsevier.com/locate/jog

Gravity tide and seasonal gravity variation at Ny-Ålesund, Svalbard in Arctic

Tadahiro Sato [a,*], Jean Paul Boy [b], Yoshiaki Tamura [a], Koji Matsumoto [a], Kazuyoshi Asari [a], Hans-Peter Plag [c,1], Olivier Francis [d]

[a] *National Astronomical Observatory of Japan, 2-12 Hoshigaoka, Mizusawa 023-0861, Japan*
[b] *Ecole et Observatoire des Sciences de La Terre, Institut de Physique du Globe, France*
[c] *Geodetic Institute of Norwegian Mapping Authority, Norway*
[d] *University of Luxembourg and European Center for Geodynamics and Seismology, Luxembourg*

Accepted 30 August 2005

Abstract

We have analyzed 4 years of gravity data (September 1999–August 2003) obtained from the superconducting gravimeter at Ny-Ålesund, Svalbard in Arctic. The tidal analysis results indicate that the time variation in amplitude and phase of the short-period gravity tides may be due to the seasonal variation of the ocean tides, especially in the semidiurnal band. The gravity residuals, which were reduced from the following three effects from the original data: (1) the observed short- and long-period tides (up to the annual Sa wave) including the loading and attraction of ocean tide, (2) the air pressure and (3) the polar motion, show clear correlation with the computed hydrological effects (i.e. the effects of soil moisture and snow) in both the amplitude and phase. However, we found that the gravity data reveal a problem in the snow model at Ny-Ålesund that was used for the computation. The vertical motion obtained from the continuous GPS measurements carried out near the gravity station shows seasonal variations that are consistent with the gravity data at least in their sign.

Keywords: Ny-Ålesund; Superconducting gravimeter; Tides; Seasonal gravity variation; Hydrology

1. Introduction

Since September 1999, Norwegian Mapping Authority (NMA) and National Astronomical Observatory of Japan are conducting continuous gravity observations with a superconducting gravimeter (SG) at Ny-Ålesund (78.93061° in latitude and 11.86717° in longitude) as the most northern observation site of Global Geodynamics Project (GGP, Crossley et al., 1999). The continuous gravity observation at this site should give us useful information on the study for gravity changes and the related geodetic problems in the polar region such as the secular changes related to post-glacial rebound, because there is rarely such a high latitude observation station as Ny-Ålesund where several kinds of observations including tide gauge and space geodetic observations are collocated with the gravimeter (Plag, 1999).

* Corresponding author. Tel.: +81 197 227137; fax: +81 197 222715.
E-mail address: tsato@miz.nao.ac.jp (T. Sato).
[1] Present address: University of Nevada, USA.

0264-3707/$ – see front matter © 2005 Elsevier Ltd. All rights reserved.
doi:10.1016/j.jog.2005.08.016

Precise investigation of the tide and the seasonal variation is important to increase the accuracy of the discussion about the topics mentioned above.

In this paper, first we will show the tidal analysis results of the 4 years data set from the beginning of the observation as a basic data to study the gravity changes at Ny-Ålesund. Then, we will discuss the seasonal gravity changes in relation to the hydrological cycle in Ny-Ålesund.

2. Gravity tides at Ny-Ålesund

2.1. SG observation and the calibration of the scale factor

The SG (GWR CT#039) is installed at the gravimeter room of the Ny-Ålesund geodetic observatory. The site is located near the edge of a steep slope of about 44 m above sea level and at about 100 m from the sea coast. Minimum digit of the A/D converter used in the data acquisition system corresponds to 0.0001 μGal (1 μGal = 10^{-8} m s^{-2}) of the apparent gravity change. The sampling interval is 1 s and its timing is locked to UTC with a GPS clock.

Scale factor of the SG (i.e. μGal/V value) has been calibrated three times during the period of 2000–2003 with the FG5 absolute gravimeters (Sato et al., 2003). We used here the weighted mean value of these three calibrations as the scale factor for our analysis (i.e. -70.54 ± 0.43 μGal/V). The data include step-like changes due to the power failure and adjustment of the position of proof mass of the SG and so on. Referred to the secular gravity change of −2.5 μGal/year in rate, which was obtained from four absolute gravity (AG) values obtained in the period of 1998–2002 (Sato et al., 2005), we have examined the magnitude of the steps, so that the coefficient of linear drift of the SG data is to be coincident with the AG rate. These steps were clearly identified and corrected: one in December 1, 1999 with 4.0 μGal, the second in September 9, 2001 with 41.6 μGal and the third in November 11, 2002 with 36.2 μGal.

2.2. Tidal analysis results for the short- and long-period tides

The software 'BAYTAP-G' (Tamura et al., 1991) and a modified version for the long-period tides were used for the analysis. For the analysis of the short-period tides, we used the 1-h data, which were sampled from the 1-min data with a digital low-pass filter with a cut-off period of 1 h. For the long-period tides (i.e. from the 4–5 days wave to the annual Sa wave), we used the trend component decomposed by the BAYTAP-G analysis and sampled at 1-day by taking the 24-h mean. The effect of the air pressure changes was estimated by an admittance factor to the local air pressure data in the BAYTAP-G analysis.

Table 1
Comparison between the observed gravity tides and the prediction

Wave	Tidal factor	Observation		Prediction	
		Amplitude (μGal)	Phase (degree)	Amplitude (μGal)	Phase (degree)
Sa	1.03 (1.52)	0.93 (1.36)	9.4 (84.1)	0.982	−0.18
Ssa	1.01 (0.48)	5.73 (2.70)	7.4 (26.7)	6.175	−0.25
Mm	1.14 (0.01)	7.34 (0.08)	−1.2 (0.7)	7.095	−1.17
Mf	1.12 (0.01)	13.57 (0.06)	−1.0 (0.3)	13.635	−1.36
Mtm	1.11 (0.02)	2.57 (0.06)	0.7 (1.3)	2.631	−1.25
Q1	1.0786 (0.0058)	2.421 (0.013)	−0.44 (0.31)	2.399	−0.75
O1	1.1498 (0.0011)	13.481 (0.012)	−1.24 (0.05)	13.238	−1.43
M1	1.16528 (0.012)	1.075 (0.011)	−1.24 (0.57)	1.067	−1.37
P1	1.1613 (0.0020)	6.335 (0.011)	1.84 (0.10)	6.391	1.00
K1	1.1508 (0.0007)	18.977 (0.011)	1.82 (0.03)	18.805	1.20
N2	0.3911 (0.0056)	0.208 (0.003)	178.28 (0.82)	0.179	183.58
M2	0.7874 (0.0011)	2.184 (0.003)	−108.12 (0.08)	2.178	−106.66
S2	1.3932 (0.0022)	1.798 (0.003)	−58.49 (0.09)	1.723	−55.97
K2	1.3857 (0.0080)	0.486 (0.003)	−59.83 (0.33)	0.434	−60.46

The predicted values show the sum effect of the body tide computed using the gravity tidal factor by Dehant et al. (1999) and the ocean tide effect computed by GOTIC2 (Matsumoto et al., 2001). Numerical values enclosed by parentheses show the root mean square errors. Phase shows the local phase lag with the plus sign.

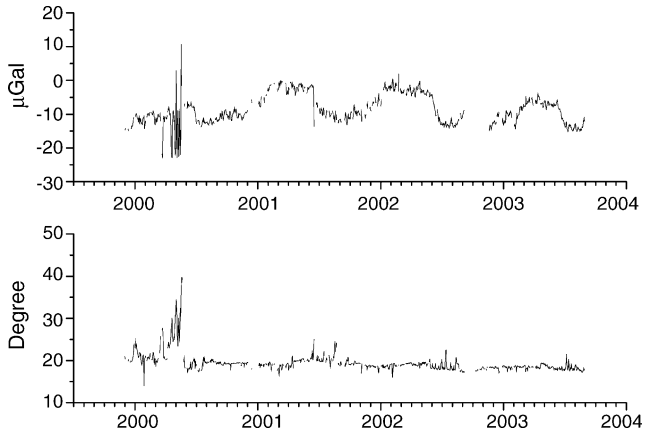

Fig. 1. Gravity residuals (top) and temperature variation of the SG room.

Table 1 shows the tidal analysis results for the 14 waves and the predicted values. The predicted values are the sum of the body tide effects computed with the gravity tidal factors of Dehant et al. (1999) and the ocean tide effects computed by GOTIC2 (Matsumoto et al., 2001). GOTIC2 computes the effect of the short-period ocean tides using the NAO.99b global ocean tide model by Matsumoto et al. (2000), which was generated by assimilating the tides obtained from TOPEX/Poseidon (T/P) satellite altimeter data with the hydrodynamic equation. For the long-period tides, it uses a pure hydrodynamic model computed by Takanezawa et al. (2001). In this computation, we used the loading Green function for the PREM earth model (Dziewonski and Anderson, 1981).

3. Gravity residuals

Fig. 1 shows the daily gravity residuals (top) after subtracting the short- and long-period gravity tides obtained by the BAYTAP analysis (i.e. up-to the monthly Mm waves in period), the predicted annual (Sa) and semiannual (Ssa) tides, the air pressure effect and the polar motion effect. The Sa and Ssa body tides were estimated by assuming 1.16 and 0° as the tidal factor and phase, respectively. To remove the annual and semiannual oceanic effects, we used the results from Sato et al. (2005), which were estimated using the monthly tide gauge data archived at the Permanent Service for Mean Sea Level of Proudman Oceanographic Laboratory of United Kingdom: 12 tide gauges covering the North Sea and the seas of the polar region. In their computation, the effect of the air pressure changes to the sea level was corrected before the convolution integral by using the data provided by the Climate Research Unit of University East Anglia of United Kingdom. The polar motion effect was estimated using the IERS polar motion data and by assuming 1.16 and 0° as the tidal factor and phase.

Due to the heat produced by the chiller used to cool down the helium compressor, the temperature increased in the SG room. By opening the doors of the observation hut, the temperature of the SG room was adjusted. Large variations are observed at around March–May in 2000. It is the effect of temperature changes of SG room. To avoid this strong temperature effect, the chiller was moved to the next building in May 2000 and panel heaters were set up in the SG room. Although the chiller was returned to the entrance room (i.e. chiller room) of the gravimeter hut in August 2002, at that moment, a fan system was introduced to control the temperature at the chiller room.

As shown in Fig. 1, after May 2000, the temperature changes at the SG room have been remarkably reduced. On the other hand, we observe a clear seasonal change in the gravity residuals. We examined the correlation between the temperature changes in the SG room and the SG data, and we have confirmed that, after May 2000, the temperature changes are not the main source of the seasonal gravity change shown in Fig. 1.

4. Discussion

4.1. Gravity tides in Ny-Ålesund

From the BAYTAP-G analysis for the data of 1-h sampling, we obtained -0.422 ± 0.004 μGal/hPa for a mean coefficient of the air pressure effect over the 4 years used in this study. This value is almost the same in magnitude

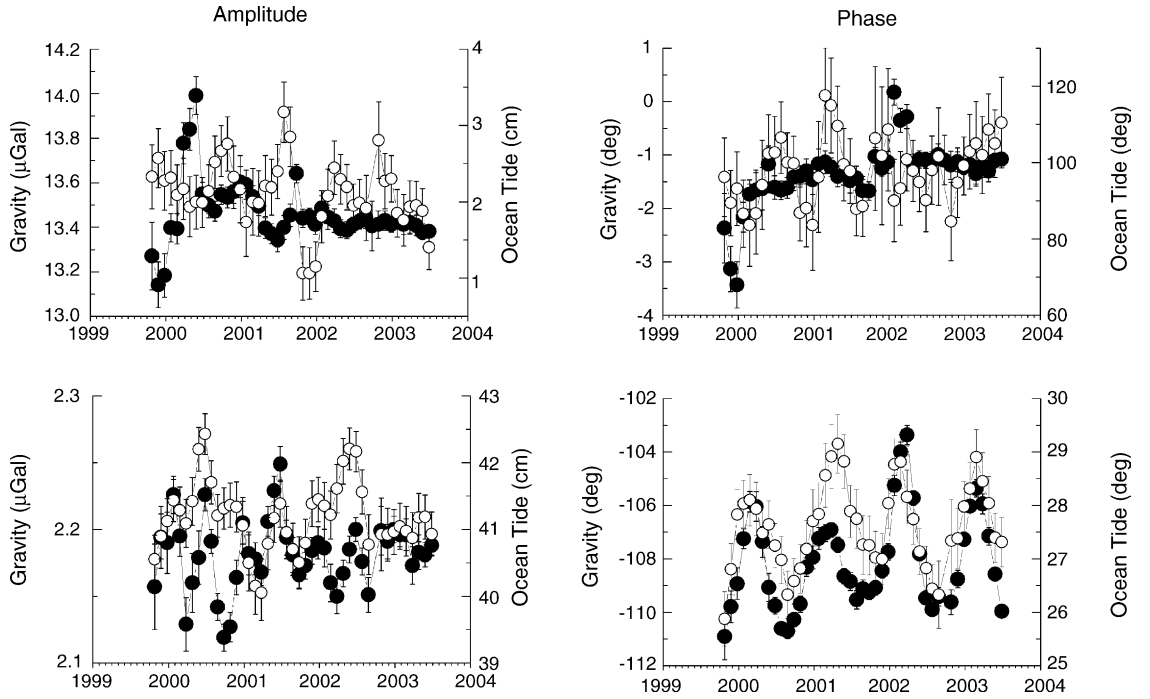

Fig. 2. Temporal variations in the tidal amplitude and phase observed from the SG and the tide gauge at Ny-Ålesund. Top: O1 wave and bottom: M2 wave. For each plot, the filled circle shows the gravity data and the open circle shows the tide gauge data.

as that from the attraction by the air mass approximated with a half-infinite plan model (i.e. −0.42 μGal/hPa). This suggests that, at the Ny-Ålesund, a site near the sea coast and in an island, most of the effect of air mass loading is compensated by an inverted barometer response in the surrounding sea.

Compared to the results by Sato et al. (2003), the observational errors shown in Table 1 are not drastically improved, even though the data length used is longer by 1 year than in the previous analysis. To examine the reason, we analyzed the time variations in amplitude and phase of the observed gravity tides. The analysis carried out by successively shifting a 3 months data window by 1 month. Fig. 2 shows the results for the O1 and M2 waves. For comparison, the similar analysis results for the tide gauge data at Ny-Ålesund are also displayed on this figure. Table 2 shows the mean amplitudes of the ocean tides obtained from the tide gauge data (data length: about 5.7 years from January 1998 to August 2003). In this table, we also show the amplitude ratio of the ocean tide effects to the body tide.

Fig. 2 and Table 2 indicate that, at Ny-Ålesund, the amplitude of the semidiurnal ocean tides is much larger than that of the diurnal tides. Moreover, while the diurnal ocean tide effect is only 2–3% of the body tide in amplitude, for the semidiurnal tide, the effect is similar in magnitude of the body tide or more than it. Reflecting this, as shown in Fig. 2, a clear coherency between the gravity and ocean tides is observed for the semidiurnal tide especially in the phase of the M2 wave. Therefore, we can say that the variation in the ocean tides is one of the major sources of the observed

Table 2
Amplitude and phase of the ocean tides obtained from the Ny-Ålesund tide gauge data

Wave	Observed ocean tide		Amplitude ratio
	Amplitude (cm)	Phase (degree)	
O1	2.05 (0.08)	98.0 (2.2)	0.032
K1	5.83 (0.08)	−99.9 (0.8)	0.023
M2	41.25 (0.07)	27.5 (0.1)	1.360
S2	15.21 (0.08)	72.6 (0.3)	1.020

Data length used for the analysis: about 5.7 years of January 1998–August 2003. Amplitude ratio: amplitude ratio of the ocean tide effect (μGal) to the body tide effect (μGal).

temporal variations in the gravity tide. At this moment, it is not clear what the mechanism of the temporal change in the ocean tide is, but we may say that, at least, it is not due to the steric changes in the sea surface layer, because very coherent changes are also observed by the SG.

On the other hand, Table 1 indicates that the prediction well recovers the observed gravity tides (i.e. within the difference less than 0.3 μGal in amplitude and 5° in phase) except for the Ssa and Sa waves. It demonstrates that the predicted values well reproduce the characteristics in the observed amplitude and phases, even though the site is located in the Arctic region where the NAO.99b global ocean tide model built in GOTIC2 is not constrained with the T/P altimeter data (i.e. covering area of T/P: less than ±66° in the latitude). Sato et al. (2003) compared the results for three waves of Mf, O1 and M2 computed by GOTIC2 with those of Bos et al. (2002), which were based on the FES98 global ocean tide model (Lefevre et al., 2000) and a local ocean tide model. The two independent results are consistent with each other within the difference of 0.05 μGal in amplitude and 30° in phase for any of the three waves, even though the ocean tide models are different in the respective computations.

4.2. Gravity residuals and the hydrology

NMA is regularly monitoring the position of Ny-Ålesund at the continuous GPS observation sites. For this paper, we used the data at two sites of NALL and NAY1, which are archived at NASA JPL (Jet Propulsion Laboratory, Heflin, 2004). The SG-, NALL- and NYA1-GPS antennas are located within 7 m in the horizontal distance. We first examine the relation of the gravity residuals and the GPS data to the air temperature changes.

The seasonal signal is the dominant component in the temperature data, therefore, for the comparison, we applied a low-pass filter of 250 days to the data and subtracted a linear trend from each of these three data sets. Fig. 3 shows the comparison. Although only the data for NALL is shown in the figure, we have confirmed that the NYA1 data also show a quite similar seasonal signal, as suggested from the correlation coefficient of 0.79 ± 0.01. Actually, the maximum differences in time domain are 0.4 cm and 2.6 months in the peak-to-peak amplitude and the phase, respectively.

The SG data and the GPS data show a clear negative correlation, although we observe a difference by year in the corresponding peak positions of these two data. One of the reasons may be due to the errors in the respective observations, but the negative correlation shown in Fig. 3 is an expected relation in the change between these two signals at least. However, the obtained correlation coefficient of -5.8 ± 0.3 μGal/cm is about two times larger than a value of -3 μGal/cm expected from the free air gradient. This suggests other sources affect the observed seasonal gravity change.

As shown in Fig. 3, positive peaks in gravity are regularly observed in the spring season when the temperature passed its negative peak and is increasing. Moreover, the negative peaks appear just at the time when the temperature gets below 0 °C. These suggest that the hydrological cycle affects the observed seasonal gravity changes. We

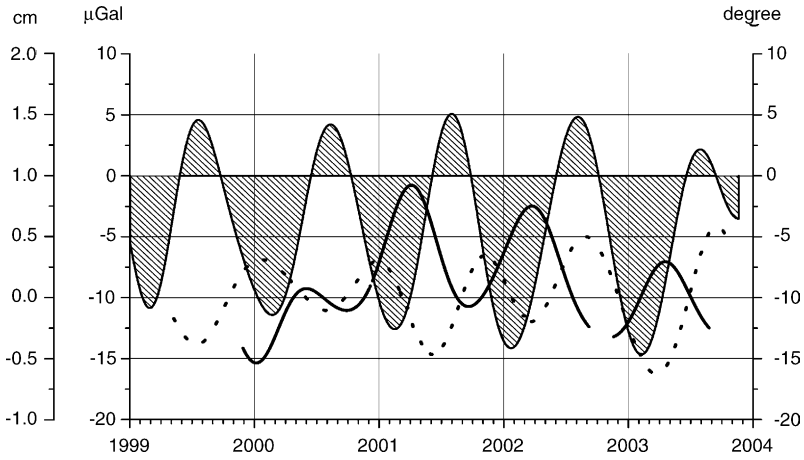

Fig. 3. Comparison of the seasonal variations derived from the three data sets of the gravity residuals (solid line), the vertical displacement (doted line) and the air temperature shown in the hatched line. The seasonal displacement derived from the GPS data at the NALL site is shown in this figure.

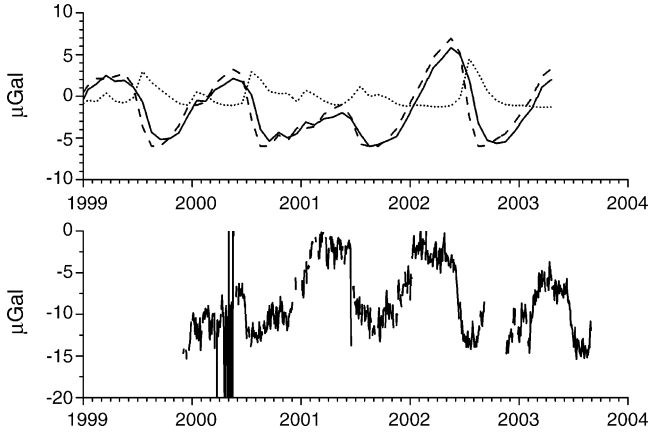

Fig. 4. Comparison between the computed gravity changes due to the hydrological effect (top) and the observed gravity residuals (bottom). In the top, thin dotted line: effect of the soil moisture, broken line: effect of the snow and solid line: sum of these two.

have estimated the gravity changes due to the effect of hydrology (i.e. the effect of snow and soil moisture) based on a hydrological "Land Dynamics model" (LaD model, Milly and Shmakin, 2002). Details of the computation method are given by Boy and Hinderer (2006) in this issue. The results for Ny-Ålesund are shown in Fig. 4. We see that hydrological model computations reproduce well a general feature of the observed seasonal cycle of the gravity changes in both amplitude and phase, thus, the gradually increasing of gravity starts on at around the end of the summer season when the air temperature becomes negative (see Fig. 3) and it continues till February–March, after gravity passes through the positive peak, gravity suddenly decreases and it reaches the negative peak at around August–September.

As described in Section 3, the quality of the SG data before May 2000 is questionable due to instability of the room temperature, but it may be worth to note the difference in the amplitude between the cycle of 2001–2002 and that of 2002–2003. Thus, while the amplitude of the observed gravity changes is not so different between these two cycles and the prediction shows a good coincidence with the observed gravity change in the later cycle, the predicted amplitude in the former cycle is too small compared with the observations. To look for possible reason for the difference in amplitude, we compared the LaD model value at Ny-Ålesund with the data of Japan Meteorological Agency (JMA). JMA run a global hydrological model for their weather forecasting by using a model similar to the LaD model. In the JMA model, the actual observed data for snow are used to constrain the model, if they are available. Ny-Ålesund corresponds to this case (Nakaegawa, personal communication, 2004). Fig. 5 shows the comparison between the LaD data and the JMA data. In this figure, both data are shown with the snow depth in unit of cm.

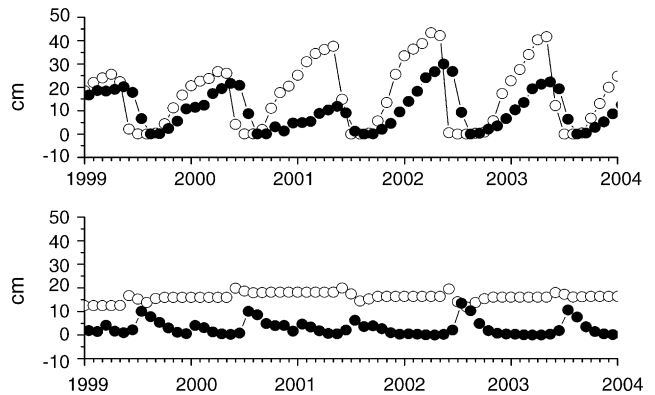

Fig. 5. Comparison between the LaD model value and the JMA data. Top: snow depth in cm and bottom: soil moisture in cm. In both plots, filled circle: the LaD model value at Ny-Ålesund and open circle: the JMA data.

Fig. 4 indicates that, in Ny-Ålesund, the effect of snow is much larger in magnitude than the effect of soil moisture, and the convolution results for the snow effect are similar to the time variations of the snow shown in Fig. 4. These indicate that the snow fall nearby has a dominant effect on the observations as in the case of the air pressure effect. Moreover, Fig. 5 shows that the maximum snow depth of the LaD model in 2001 is about three times smaller than that of the JMA data. Therefore, we can point out that the error in the LaD model is the main reason for the difference between the observation and the hydrological prediction in the 2001–2002 period. We estimated the correlation between the observed gravity residuals and the sum of the snow and soil moisture data shown in Fig. 5. The linear regression coefficients are 0.14 ± 0.08 and 0.20 ± 0.03 μGal/cm for the LaD model and the JMA data, respectively, supporting the fact mentioned above.

5. Conclusions

The residual gravity signals observed at Ny-Ålesund show a clear seasonal change, and most of the temporal variation can be explained as the effect of hydrology. However, we also found differences, especially in their amplitudes. From a comparison between the LaD model by Milly and Shmakin (2002) used for the prediction and the data of JMA, we pointed out that main source of the difference in the amplitude may be due to inaccurate snow modeling in the LaD model around Ny-Ålesund. Our study gives a good example that ground gravity observations can bring useful information to improve the accuracy of hydrological modeling. Our comparison results also show that gravity measurements with SGs can be a useful tool to improve the accuracy of the ground validation/calibration of the space gravity satellite (eg. GRACE).

Acknowledgements

We acknowledge here the excellent support of the staff of Statens Kartverk and the local Kingsbay Kull Company. Dr. Nakaegawa kindly presented the JMA hydrological data at Ny-Ålesund. A part of the observations was supported by several grants from the Large Scale Facility for Arctic Environmental Research, which was funded by the European Commission under Contracts ERBFMGECT950065 and HPRI-CT-1999-00057. The SG observation at Ny-Ålesund was also supported by Grants in Aid for Scientific Research of the Ministry of Education, Culture, Sport, Science and Technology of Japan (MEXT): Nos. 09NP1101, 13440135 and 1430132. The authors thank anonymous reviewers for their valuable comments to revise the manuscript.

References

Bos, M.S., Baker, T.F., Rothing, K., Plag, H.-P., 2002. Testing ocean tide models in the Nordic seas with tidal gravity observations. Geophys. J. Int. 150, 687–694.

Boy, J.-P., Hinderer, J., 2006. Study of the seasonal gravity signal in superconducting gravimeter data. J. Geodynamics 41 (1–3), 227–233.

Crossley, D., Hinderer, J., Casula, G., Francice, O., Hsu, H.-T., Imanishi, Y., Jentzsch, G., Kääriäinen, J., Merriam, J., Meurers, B., Neumeyer, J., Richter, B., Shibuya, K., Sato, T., van Dam, T., 1999. Network of superconducting gravimeters benefits a number of displines, EOS. Trans. Am. Geophys. Union 80 (11), 125–126.

Dehant, V., Defraigne, P., Wahr, J.M., 1999. Tides for a convective Earth. J. Geophys. Res. 104 (B1), 135–158.

Dziewonski, A.D., Anderson, D.L., 1981. Preliminary reference Earth model. Phys. Earth Planet. Int. 25, 297–356.

Heflin, M.B., 2004. GPS time series, http://sideshow.jpl.nasa.gov/mbh/series.html/.

Lefevre, F., Lyard, F.H., Le Provost, C., 2000. FES98: a new global tide finite element solution independent of altimetry. Geophys. Res. Lett. 27 (17), 2717–2720.

Matsumoto, K., Takanezawa, T., Ooe, M., 2000. Ocean tide models developed by assimilating TOPEX/POSEIDON altimeter data into hydrodynamical model: a global model and a regional model around Japan. J. Oceanogr. 56, 567–581.

Matsumoto, K., Sato, T., Takanezawa, T., Ooe, M., 2001. GOTIC2: a software for computation of oceanic tidal loading effect. J. Geodetic Soc. Jpn. 47 (1), 243–248.

Milly, P.C.D., Shmakin, A.B., 2002. Global Modeling of Land Water and Energy Balances. Part I: The Land Dynamics (LaD) Model.

Plag, H.-P., 1999. Measurements of vertical crustal motion in Europe by VLBI-Station report for Ny-Ålesund, Norwegian Mapping Authority. In: Schlueter, W., Hass, R. (Eds.), Proceedings of the 13th Working Meeting of European VLBI for Geodesy and Astrometry, pp. 65–77.

Sato, T., Tamura, Y., Matsumoto, K., Asari, K., Plag, H.-P., van Dam, T.M., Francis, O., 2003. Comparison between modeled and observed gravity tidal parameters at Ny-Ålesund, Svalbard. In: Francis, O., Van Dam T. (Eds.), Proceedings of Instrumentation and Metrology (IGM-2002), Cahiers du Centre Européen de Géodynamique et de Séismologie, vol. 22, pp. 143–148.

Sato, T., Okuno, J., Hinderer, J., MacMillan, D.S., Plag, H.-P., Francis, O., Falk, R., Fukuda, Y., 2005. A geophysical interpretation of the secular displacement and gravity rates observed at Ny-Ålesund, Svalbard in the Arctic—effects of post-glacial rebound and present-day ice melting, Geophys. J. Int., submitted for publication.

Takanezawa, T., Matsumoto, K., Ooe, M., Naito, I., 2001. Effects of the long-period ocean tides on Earth rotation, gravity and crustal deformation predicted by global barotropic model—periods from Mtm to Sa. J. Geodetic Soc. Jpn. 47 (1), 545–550.

Tamura, Y., Sato, T., Ooe, M., Ishiguro, M., 1991. A procedure for tidal analysis with a Bayesian information criterion. Geophys. J. Int. 104, 507–516.